

CAMPAIGN FOR HYPERSPECTRAL DATA VALIDATION IN NORTH ATLANTIC COASTAL WATERS

Oudijk, A.E.¹, Hasler, O.¹, Øveraas, H.¹, Marty, S.², Williamson, D. R.^{1,3}, Svendsen, T.¹, Berg, S.¹, Birkeland R.¹, Halvorsen, D. Ø.¹, Bakken, S.^{1,3}, Henriksen, M. B.¹, Alver, M. O.¹, Johnsen, G.¹, Johansen, T. A.¹, Stahl, A.¹, Kvaløy, P.¹, Dallolio, A.^{1,3}, Majaneva, S.¹, Fragoso, G. M.¹, Garrett, J. L.¹

¹Norwegian University of Science and Technology (NTNU), Trondheim, Norway

²Norwegian Institute for Water Research (NIVA), Oslo, Norway

³SINTEF Ocean, Trondheim, Norway

ABSTRACT

The high photosynthetic productivity of the Mausund bank on the coast of mid-Norway has given the area important economic and ecologic value. Monitoring chlorophyll-a (chl-a) production can assist in managing the local aquaculture and ecosystem. Hyperspectral imagers (HSIs), with frequent revisit times when used on a small satellite, have the potential to detect chl-a over large regions. Moreover, our hypothesis is that HSIs can classify spectral signatures of different functional groups of plankton. The data must, however, first be validated to be interpreted in accordance with *in situ* data.

Recently, a HSI validation campaign was performed. HSIs on a small satellite and drones, unmanned surface and underwater vehicles with chl-a detectors, and numerical simulations were used to monitor local phytoplankton blooms. These measurements were validated with *in situ* water sampling. Each measurement technique and an outline of the campaign is described, showing the feasibility of such a coordinated mission.

Index Terms— Marine Biology, Water Sampling, Remote Sensing, CubeSat, Marine robots

1. INTRODUCTION

The Mausund bank, located along the coast of mid-Norway, and the waters to its east (Frohavet) are a biodiversity-rich spot with nearly year-round high levels of primary production [1]. Because of the high productivity, these waters are particularly attractive for many activities, including ecotourism, fishing, and aquaculture-related business, which boost the local economy [2]. The important ecologic and economic value of Frohavet drives an interest in monitoring the area, in particular chlorophyll-a (chl-a) concentrations to detect algae blooms.

This research was funded by the Research Council of Norway and industry partners through grants number AMOS (223254), MASSIVE (270959), MoniTare (315514), Nansen Legacy (276730), AILARON (262741), HYPSCI (325961), SeaBee (296478), value chain for offshore aquaculture (328674), the European Commission (Nautilus), and the EEA bilateral ELO-Hyp project funded by Norway Grants 2014-2021 contract nr. 24/2020.

Ocean color can be used to determine chl-a content [3]. Hyperspectral imaging is one possible technique to measure ocean color and calculate chl-a content [3]. However, there is some uncertainty regarding how accurately different cameras can estimate parameters such as chl-a content. For example, detecting blooms with hyperspectral data in large lakes does not give unambiguous results, possibly because the spectral reflectance does not have an evident relation with chl-a concentrations [4, 5]. A question arises: how much do hyperspectral imagers (HSIs) contribute to the environmental monitoring and how can they be utilized?

To determine what type and what accuracy of information can be inferred from hyperspectral images, the following techniques are exploited in this campaign: (1) A Specim AFX10 HSI mounted on a drone, (2) the do-it-yourself HSI v4 mounted on a drone [6], (3) radiometric measurements, (4) the AutoNaut, a wave-propelled Unmanned Surface Vehicle (USV) with oceanographic instrumentation, (5) an autonomous underwater vehicle (AUV) with silhouette camera (SilCam) imaging system, (6) water sampling, (7) numerical simulations using the SINMOD model, and (8) the HYPerspectral Smallsat for ocean Observation CubeSat (HYPSO-1) [7, 8]. The research questions that motivated the mission are the following:

1. How much spectral consistency is there between the different HSIs?
2. How well do the HSIs measure ocean color?
3. How well can the different HSIs be used to estimate chl-a content?
4. How well can time-series from HSIs on a small satellite monitor ecosystem dynamics?
5. How well do numerical simulations (SINMOD) match with observations over time?
6. How can hyperspectral images be combined with other sensing techniques?

1.1. Mission Timeline

The mission consists of two phases. In Phase I, all eight techniques were used over a time span of 36 hours, see left of

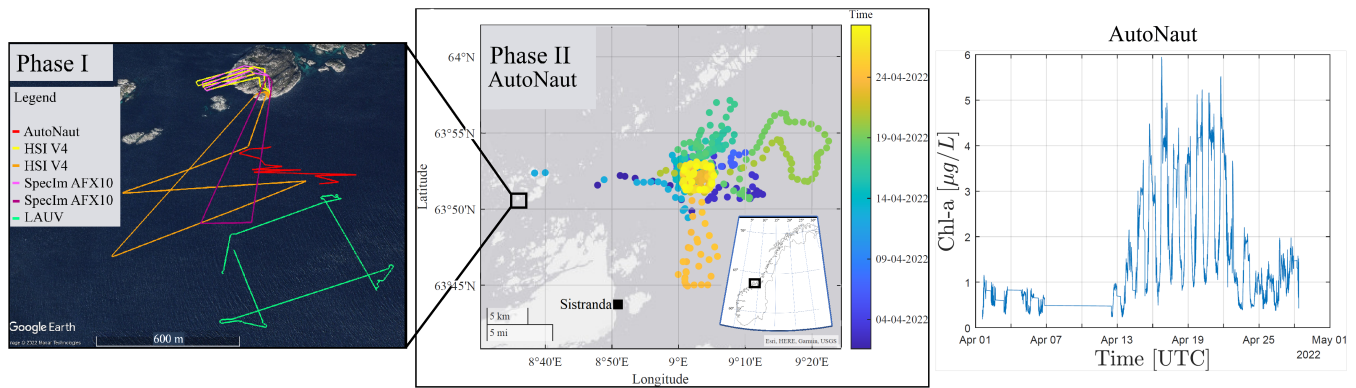


Fig. 1. During Phase I, the AutoNaut, HSI v4, Specim, and the LAUV operated in a small area over 36 hours. The paths they traveled are plotted on the left. In Phase II, the AutoNaut, HYPSO-1, and occasional water samples persisted. The routes of the AutoNaut in the period of April 1 to April 27 are shown along with the measured chl-a concentration. The occasional water samples are taken in Sistranda. HYPSO-1 is monitoring the full area.

Fig. 1. The goals of Phase I are to test what level of detail can be observed with the HSIs (research questions (1), (2), (3)), and to explore how the different measurement techniques can complement each other (research question (6)). In addition to two excursions during the day, water sampling and the underwater vehicle were also deployed at night to study chl-a dynamics.

In Phase II, the AutoNaut, SINMOD predictions, HYPSO-1, and occasional water samples persisted. The goal of Phase II is to validate HYPSO-1's and SINMOD's capacity to track changes in the coastal environment over time (research questions (4) and (5)). The frequency in which the measurements of the techniques occurred in Phase II can be seen in Fig. 2. Daily HYPSO-1 captures of Frohavet were not possible, due to scheduling and other tasks for the satellite. Moreover, some captures were fully covered in clouds or overexposed. In Fig. 2, the timeline of captures with decent exposures and no cloud coverage can be seen (dark blue), along with the captures that can be partly used for data processing, due to partly cloud coverage (light blue).

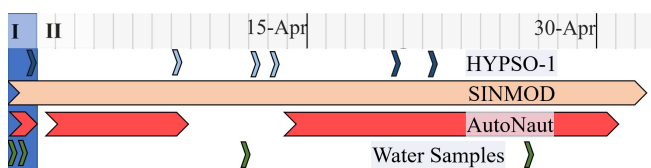


Fig. 2. Timeline showing an overview of when samples from the different measurement techniques were acquired. In phase I, all measurement techniques from Section 2 were used. HYPSON-1 takes daily measurements, but only captures containing decent exposures and no cloud coverage (dark blue) and partly cloud coverage (light blue) are shown.

1.2. Target Area Description

In Phase I, the measurements are centered in the waters around Mausund Archipelago, located west of Frohavet (Fig. 1). This area is comprised by a shallow bank with numerous small islands. The combination of shallow and irregular bathymetry and complex circulation contribute to its high primary productivity [9]. Internal waves located offshore promote the lift of Atlantic nutrient-rich waters that occasionally intrude the bank. Strong winds and tidal currents allow mixing of the water column, and make nutrients available for phytoplankton.

These phenomena contribute to a significant and varied ecosystem. Large phytoplankton (diatom chains) dominate the spring bloom and are a valuable source of food for the abundant zooplankton community dominated by copepods in spring-summer. A mixed assemblage of diatoms, coccolithophores and dinoflagellates occurs in the fall bloom as strong winds reintroduce nutrients to the surface [10]. The high abundance of copepods in this region serves as direct or indirect food to the upper trophic levels, such as birds and fish [9].

The same phenomena which make the region so rich also complicate the efforts to monitor it. The combination of shallow, irregular bathymetry and complex hydrodynamics in this area give rise to limitations to the measurement techniques. For example, it is challenging for the USV to operate autonomously in shallow areas with complex circulation. Similarly, gathering water samples is labour intensive and contains only point measurements, although it is crucial for verifying the findings of the other techniques. While HSIs have the potential to evade some of these difficulties, by flying above the water, reflections from the seabed at shallow waters should be accounted for.

2. MEASUREMENT TECHNIQUES

2.1. Hyperspectral imaging

Three HSIs were used during the mission. First, a Specim AFX10 was carried on a drone (DJI M600). It records 448 bands in the range of 400–1000 nm, with a 1024 pixel swath width and a 38 degree field of view. One example Red-Green-Blue (RGB) composite of the Specim measurement gathered during the mission was constructed using center wavelengths of 648 nm, 548 nm, 448 nm (red, green, blue). The RGB composite and two example spectra of rocks and water can be seen in Fig. 3. The camera is flown at an altitude of 150 m with a 50 frames-per-second (fps) sampling rate and with $2\times$ spatial and spectral binning.

The second HSI that was carried on a drone during the mission is the Sigernes HSI v4, which is made from commercial off-the-shelf (COTS) components and described and validated in [6, 11]. The low weight of the Sigernes HSI v4 makes it a good candidate for extended operations and smaller drones. It has a spectral range of 400–800 nm, a swath angle of 5.36° , and uses a UI-5360CP-NIR imaging sensor from (Imaging Development Systems) IDS with a resolution of 2048×1088 pixels. The spectral pixels were binned, resulting in 136 spectral bands. In addition to the Sigernes HSI v4, a mini-spectrometer was used to measure the irradiance and the spectrum of the sky above the drone path. The data of this spectrometer will be used in post-processing to do atmospheric corrections of the hyperspectral data.

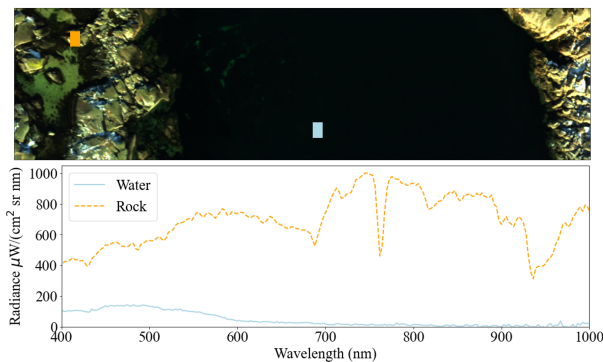


Fig. 3. Image captured during the pink flight in Fig. 1 by the Specim camera (top), the image covers an area of approximately 50×200 m. Two sample spectra of water (blue dot) and rock (orange dot) are shown on the bottom.

The third HSI used in this campaign is the HSI v6, which is part of the payload of the HYPSON-1 CubeSat [7]. The HYPSON-1 has been in orbit at a 540 km altitude from Earth since January 2022. During this campaign the satellite is operated so that daily hyperspectral images are attempted, with a focus on Frohavet. The HSI v6 allows to observe 124 spectral bands in the range of 400–800 nm, and is specifically designed for the HYPSON-1 [8]. A RGB composite of one of the captures by HYPSON-1 over Frohavet can be seen in

Fig. 4. The RGB composite was constructed using the center wavelengths of 630.2 nm, 564.0 nm, and 483.4 nm (red, green, blue).

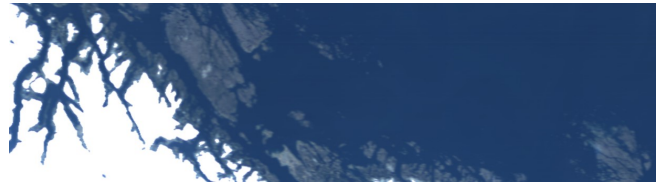


Fig. 4. Image captured by the HYPSON-1 satellite on the 19th of April 2022. White areas are overexposed. North points towards the right in the image, Frohavet is located in the centre. The image covers an area of approximately 70×250 km.

In addition to the three HSIs, radiometric measurements, with an instrument similar to that presented in [12], were performed on the water where the HSIs were deployed during Phase I. During the data processing after this campaign, the agreement between the three different hyperspectral cameras will be determined, and also compared with multi-spectral data products from global Earth Observation (EO) satellites.

2.2. Other robotic platforms

The long-endurance unmanned surface vehicle AutoNaut [13] participated in both phases of the campaign. Unlike common marine surface vehicles, the AutoNaut uses the waves to generate its forward propulsion. Moreover, three deck-mounted solar panels provide the energy, harvested in the onboard battery bank, used to power the navigation and scientific instrumentation. The scientific payload consists of a Conductivity, Temperature and Depth sensor (CTD), Acoustic Doppler Current Profiler (ADCP), oxygen optode, fluorometer (for chl-a), radiometer and weather station. During the deployment, the USV continuously measured chl-a fluorescence, turbidity, sea surface temperature, salinity and oxygen saturation. The AutoNaut is part of the ensemble of *in situ* agents in the HYPSON observational pyramid [14]. The path that the AutoNaut navigated autonomously in Phases I and II can be seen in Fig. 1. In addition, the measured chl-a concentration clearly shows an increase of chl-a concentration in the middle of April. Moreover, the day- and night-peaks of the chl-a can be seen.

The AUV used in this study was an LAUV (Light Autonomous Underwater Vehicle) [15]. It carries a range of payload sensors, of which the most relevant to this study are a CTD, fluorometer, salinity and turbidity sensors, and a Sil-Cam [16] for particle imaging. During this campaign two missions were carried out with the LAUV, one during daylight and one shortly after dusk. The daylight mission took around 45 minutes, during which time the vehicle travelled approximately 3.5 km, and the track of this mission can be seen in Fig. 1. The night mission took 1 hour, 5 minutes and covered a distance of 5.6 km. In each missions a maximum depth of 42 m was reached, with a mean depth of 15 m.

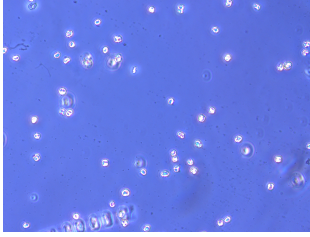


Fig. 5. The dinoflagellate *Gymnodinium* spp.

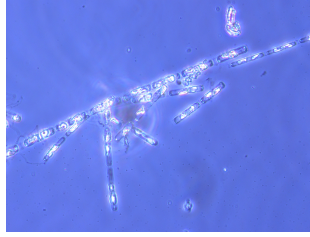


Fig. 6. The diatom *Skeletonema* spp. The length of one cell is approximately 15 μm .

The SilCam recorded images while the vehicle was conducting transects underwater but not while at the surface, recording around 24 000 images in total. All other sensors recorded continuously.

2.3. Water Sampling

Water samples for pigment concentrations (*chlorophylls* and *carotenoids*) and environmental DNA (eDNA) to assess the in situ phytoplankton community composition were collected once during daylight and once one shortly after dusk, at 4 depths: surface, 15 m, 25 m and 50 m during Phase I, at the locations that can be seen in Fig. 1. Based on sampling conducted in Sistranda just before Phase I, we could see that the dinoflagellate *Gymnodinium* spp., see Fig. 5 bloomed just before Phase I (Fragoso, unpublished data). However, the *Gymnodinium* spp. bloom might have collapsed during the time of sampling, as the mixed layer depth was quite deep, which reduced the amount of light for the phytoplankton.

During Phase II of the mission, occasional water samples will be taken every two weeks in the period of March-June, at Sistranda, see Fig. 1. During Phase II of the mission, the diatom *Skeletonema* spp. see Fig. 6 can be the dominating phytoplankton species as its bloom has been recorded in mid-April in the bi-weekly sampling in Sistranda (Fragoso, unpublished data).

2.4. SINMOD model

Numerical simulations using the SINMOD model [17, 18] are performed continuously to estimate spatial-temporal data from the physics and biology of the Norwegian coast with a 2 day forecast horizon. The SINMOD model is a 3-dimensional, hydrodynamic model, based on the Navier-Stokes equations and advection-diffusion equations for salinity and temperature [17], and an ecological model developed for the Norwegian and Barents seas [18]. Outputs of the model are hydrodynamic properties e.g., current velocity, salinity and temperature, but also biological properties, e.g. production of diatoms, flagellates or chl-a concentrations. For this campaign the main interest is in detecting chl-a and phytoplankton classification, to compare the gathered hyper-

spectral data with the findings from the model. Our research hypothesis is that the hyperspectral image data from the HYPISO satellite has significant potential for improving the accuracy of the SINMOD model through data assimilation. The output of chl-a from the SINMOD grid can be seen in Fig. 7.

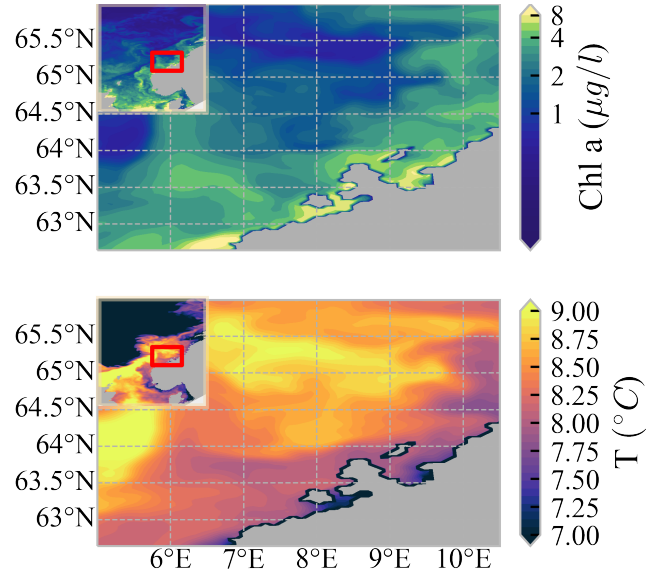


Fig. 7. SINMOD values for chl-a and surface temperature on the 29th of April 2022. The horizontal resolution of the model domain is 4 km.

3. DISCUSSION AND CONCLUSIONS

As of the time of writing, the mission is still ongoing, and the data are being processed. We collected the following data of the Frohavet target area:

1. Two drone flights with the Specim HSI.
2. Two drone flights with the Sigernes HSI v4
3. Radiometric measurements concurrent with the drone flights
4. About a month of continuous measurements by the AutoNaut
5. Daylight and dusk measurement series of approximately an hour of underwater chlorophyll concentrations, temperature and particle images by the LAUV
6. Water samples during daylight and at dusk at 4 different depths, in Phase I. And 4 more water samples taken every two weeks
7. Continuous numerical simulations from the SINMOD model
8. Several captures of the full Frohavet area with the HSI mounted on the HYPISO-1 (daily observation was not possible due to cloud coverage, scheduling, and other tasks for the satellite).

The datasets of the HSIs complement the datasets gath-

ered by the other instruments. For example, HSIs can fly over more shallow areas where the LAUV and AutoNaut cannot measure, the LAUV and AutoNaut can measure after sunset, and the LAUV allows to measure at larger depths than possible with the HSIs. Examples of collaborative interactions between the agents include the possibility that the HSIs scan a large area in order to direct the LAUV and AutoNaut to measure at interesting target locations within this large area. It is of interest in future work to focus on time-series hyperspectral imaging to assess the performance of the HSIs, as the illumination and other environmental issues change over time. Processing these data sets will help to find how hyperspectral cameras can be used to understand oceanic phenomena better. This paper documents the feasibility of this mission.

4. REFERENCES

- [1] R. Sætre, *The Norwegian coastal current: oceanography and climate*, Akademika Pub, 2007.
- [2] H. Ervik, T. E. Finne, and B.M. Jenssen, “Toxic and essential elements in seafood from Mausund, Norway,” *Environmental Science and Pollution Research*, vol. 25, no. 8, pp. 7409–7417, 2018.
- [3] Z.P. Lee et al., *Remote Sensing of Inherent Optical Properties: Fundamentals, Tests of Algorithms, and Applications.*, International Ocean Colour Coordinating Group (IOCCG), 2006.
- [4] L. Feng, Y. Dai, Xu. Hou, Y. Xu, J. Liu, and C. Zheng, “Concerns about phytoplankton bloom trends in global lakes,” *Nature*, vol. 590, no. 7846, pp. E35–E47, 2021.
- [5] E. Spyrakos, R. O’Donnell, P.D. Hunter, C. Miller, M. Scott, S.G.H. Simis, C. Neil, C.C.F. Barbosa, C.E. Binding, S. Bradt, et al., “Optical types of inland and coastal waters,” *Limnology and Oceanography*, vol. 63, no. 2, pp. 846–870, 2018.
- [6] F. Sigernes, M. Syrjäsuo, R. Storvold, J. Fortuna, M. E. Grøtte, and T. A. Johansen, “Do it yourself hyperspectral imager for handheld to airborne operations,” *Optics express*, vol. 26, no. 5, pp. 6021–6035, 2018.
- [7] M.E. Grøtte, R. Birkeland, E. Honoré-Livermore, S. Bakken, J.L. Garrett, E.F. Prentice, F. Sigernes, M. Orlandić, J. T. Gravdahl, and T. A. Johansen, “Ocean color hyperspectral remote sensing with high resolution and low latency—the HYPISO-1 Cubesat mission,” *IEEE Transactions on Geoscience and Remote Sensing*, vol. 60, pp. 1–19, 2021.
- [8] E.F. Prentice, M.E. Grøtte, F. Sigernes, and T. A. Johansen, “Design of a hyperspectral imager using COTS optics for small satellite applications,” in *International Conference on Space Optics—ICSO 2020*. International Society for Optics and Photonics, 2021, vol. 11852, p. 1185258.
- [9] G.M. Fragoso, E.J. Davies, I. Ellingsen, M.S. Chauton, T. Fossum, M. Ludvigsen, K.B. Steinhovden, K. Rajan, and G. Johnsen, “Physical controls on phytoplankton size structure, photophysiology and suspended particles in a norwegian biological hotspot,” *Progress in Oceanography*, vol. 175, pp. 284–299, 2019.
- [10] G. M. Fragoso, G. Johnsen, M.S. Chauton, F. Cottier, and I. Ellingsen, “Phytoplankton community succession and dynamics using optical approaches,” *Continental Shelf Research*, vol. 213, pp. 104322, 2021.
- [11] J. Fortuna and T. A. Johansen, “A lightweight payload for hyperspectral remote sensing using small UAVs,” in *9th Workshop on Hyperspectral Image and Signal Processing: Evolution in Remote Sensing, Amsterdam*, 2018.
- [12] Z. Lee, N. Pahlevan, Y. Ahn, S. Greb, and D. O’Donnell, “Robust approach to directly measuring water-leaving radiance in the field,” *Applied Optics*, vol. 52, no. 8, pp. 1693–1701, 2013.
- [13] A. Dallolio, B. Agdal, A. Zolich, J.A. Alfredsen, and T.A. Johansen, “Long-endurance green energy autonomous surface vehicle control architecture,” in *OCEANS 2019 MTS/IEEE SEATTLE*. IEEE, 2019, pp. 1–10.
- [14] A. Dallolio, G. Quintana-Diaz, E. Honoré-Livermore, J.L. Garrett, R. Birkeland, and T.A. Johansen, “A satellite-USV system for persistent observation of mesoscale oceanographic phenomena,” *Remote Sensing*, vol. 13, no. 16, pp. 3229, 2021.
- [15] L. Madureira, A. Sousa, J. Braga, P. Calado, P. Dias, R. Martins, J. Pinto, and J. Sousa, “The light autonomous underwater vehicle: Evolutions and networking,” in *2013 MTS/IEEE OCEANS-Bergen*. IEEE, 2013, pp. 1–6.
- [16] E.J. Davies, P.J. Brandvik, F. Leirvik, and R. Nepstad, “The use of wide-band transmittance imaging to size and classify suspended particulate matter in seawater,” *Marine Pollution Bulletin*, vol. 115, no. 1, pp. 105–114, 2017.
- [17] D. Slagstad and T.A. McClimans, “Modeling the ecosystem dynamics of the barents sea including the marginal ice zone: I. Physical and chemical oceanography,” *Journal of Marine Systems*, vol. 58, no. 1-2, pp. 1–18, 2005.
- [18] P. Wassmann, D. Slagstad, C.W. Riser, and M. Reigstad, “Modelling the ecosystem dynamics of the barents sea including the marginal ice zone: Ii. Carbon flux and interannual variability,” *Journal of Marine Systems*, vol. 59, no. 1-2, pp. 1–24, 2006.